AIP | Journal of Applied Physics

Hightemperature annealings of Sb and Sb/B heavily implanted silicon wafers studied by near grazing incidence fluorescence extended xray absorption fine structure

C. RevenantBrizard, J. R. Regnard, S. Solmi, A. Armigliato, S. Valmorri et al.

Citation: J. Appl. Phys. 79, 9037 (1996); doi: 10.1063/1.362636
View online: http://dx.doi.org/10.1063/1.362636
View Table of Contents: http://jap.aip.org/resource/1/JAPIAU/v79/i12
Published by the American Institute of Physics.

Related Articles

Interaction of n-type dopants with oxygen in silicon and germanium
J. Appl. Phys. 112, 073706 (2012)

A mathematical model for void evolution in silicon by helium implantation and subsequent annealing process
J. Appl. Phys. 112, 064302 (2012)

Multiple implantation and multiple annealing of phosphorus doped germanium to achieve n-type activation near the theoretical limit
Appl. Phys. Lett. 101, 112107 (2012)

Electronegativity and doping in semiconductors
J. Appl. Phys. 112, 046101 (2012)

High phosphorous doped germanium: Dopant diffusion and modeling
J. Appl. Phys. 112, 034509 (2012)

Additional information on J. Appl. Phys.

Journal Homepage: http://jap.aip.org/
Journal Information: http://jap.aip.org/about/about_the_journal
Top downloads: http://jap.aip.org/features/most_downloaded
Information for Authors: http://jap.aip.org/authors

ADVERTISEMENT

Downloaded 15 Nov 2012 to 155.69.4.4. Redistribution subject to AIP license or copyright; see http://jap.aip.org/about/rights_and_permissions

High-temperature annealings of Sb and Sb/B heavily implanted silicon wafers studied by near grazing incidence fluorescence extended x-ray absorption fine structure

C. Revenant-Brizard[a] and J. R. Regnard[b]
Département de Recherche Fondamentale sur la Matière Condensée/SP2M, CEA/Grenoble, 17 rue des Martyrs, 38054 Grenoble Cedex 9, France

S. Solmi, A. Armigliato, and S. Valmorri
CNR-Istituto LAMEL, Via P. Gobetti, 101 40129 Bologna, Italy

C. Cellini and F. Romanato
INFM, Dipartimento di Fisica dell'Università, Via Marzolo 8, 35131 Padova, Italy

(Received 18 January 1996; accepted for publication 6 March 1996)

The local atomic environment of the Sb dopant in 2 and 5×10^{16} ions/cm^2 implanted Si samples has been studied by near grazing incidence fluorescence extended x-ray absorption fine structure at different stages of the Sb deactivation process. The annealings were performed at high temperature (900–1000 °C) during various periods: 30 s–4 h. The Sb out-diffusion and the high percentage of Sb precipitates are put into evidence especially for Sb-only implanted samples. The comparison of the Sb and B codiffusion data with the corresponding ones obtained by the diffusion of Sb alone revealed several anomalous effects due to dopant interaction. Moreover, a simulation program including dopant precipitation and donor–acceptor pairing allows us to foresee most of the anomalous phenomena occurring in high-concentration codiffusion experiments. *© 1996 American Institute of Physics.* [S0021-8979(96)00812-2]

I. INTRODUCTION

The knowledge of the properties of silicon highly implanted with atoms of the groups III/V is of great interest for the microelectronics technology. In the case of Sb, a commonly used dopant, the maximum equilibrium concentration of Sb atoms in substitutional position, and hence electrically active, is of about 2×10^{19} atoms/cm^3 at 1000 °C.[1,2] Above this concentration, Larsen *et al.* suggested the coexistence of precipitates and vacancy complexes.[3] Moreover, it has been shown from a previous extended x-ray absorption fine structure (EXAFS) study[4] that these vacancy complexes SbV_2 (V: vacancy) are already present after laser annealing in the 5×10^{16} Sb/cm^2 case and that the coimplantation with B reduces the precipitation of Sb particles, by forming Sb–B complexes. In this study, the local environment of the Sb dopant in 2 and 5×10^{16} ions/cm^2 samples has been studied by near grazing incidence fluorescence EXAFS. Different stages of the Sb deactivation have been analyzed in samples annealed at high temperatures (900–1000 °C) during various periods: from 30 s to 4 h. Furthermore, the influence of B on the Sb environment has been studied in Sb–B coimplanted samples.

II. EXPERIMENT

A. Samples

The implantation of Sb and the coimplantation of Sb and B have been investigated in ⟨100⟩ Si monocrystalline wafers. Two implantation doses have been studied: 2 and 5×10^{16} ions/cm^2. In each coimplanted sample, the Sb and B doses are of the same order of magnitude to maximize the coimplantation effect.[5] The Sb^+ and B^+ ions have been implanted at 160 and 30 keV, respectively.

A thermal annealing at high temperature is necessary to recrystallize the implanted material. Thermal annealings of the implanted samples have been performed in a nitrogen atmosphere with 10% oxygen at a temperature of 900 °C (unless mentioned at 1000 °C) during various periods: from 30 s to 4 h. During this thermal treatment, an amorphous silicon oxide layer is formed on the Si surface.

B. Ion-beam techniques

The B and Sb concentration profiles were measured by secondary-ion-mass spectroscopy (SIMS) with a CAMECA IMS-4f spectrometer at the Physics Department of Padova University (Italy). A 5.5 keV O^{2+} beam rastered over a 250×250 μm^2 area was used for sputtering while the positive secondary-ion signals were collected from the 60-μm-diam central area. The erosion time to depth conversion was obtained with a Tencor Alpha-Step 200 stylus profilometer which was used to measure the height of the sputtering crater. The secondary-ion yields were converted into atomic concentrations by using the Sb and B dose data deduced from Rutherford backscattering (RBS) and nuclear reaction analysis (NRA) measurements, respectively. In fact, in all samples the maximum concentrations are of the order of 1 at. % and the conversion obtained by conventional low-dose ion-implanted calibration standards is affected by matrix effects. The RBS experiments have been performed by using a 2.0 MeV $^+$He beam at grazing emergence detection angles in order to obtain a depth resolution better than 20 nm.

[a]Electronic mail: brizard@cea.fr
[b]Also with: University Joseph Fourier, B. P. 53 X, 38041 Grenoble Cedex, France.

Downloaded 15 Nov 2012 to 155.69.4.4. Redistribution subject to AIP license or copyright; see http://jap.aip.org/about/rights_and_permissions

TABLE I. Structural parameters obtained from the EXAFS spectra N_{Si} (N_{Sb}) is the number of Si (Sb) nearest neighbors (NN); R_{Si} (R_{Sb}) is the NN Sb–Si (Sb–Sb) distance. The expression $2\sigma^2_{Si}$ ($2\sigma^2_{Sb}$) is the Si (Sb) Debye–Waller factor. The coordination numbers are given with an accuracy of ±10%, the distances with an accuracy of ±0.02 Å and the Debye–Waller factors with an accuracy of ±0.001 Å^2.

	Si neighbors (first shell)			Sb neighbors (first shell)		
Samples	N_{Si}	R_{Si} (Å)	$2\sigma^2_{Si}$ (Å^2)	N_{Sb}	R_{Sb} (Å)	$2\sigma^2_{Sb}$ (Å^2)
2Sb/900 °C						
15 min	0.4	2.57	0.006	2.8	2.90	0.012
1 h	0	⋯	⋯	3	2.90	0.014
4 h	0.2	2.60	0.009	2.7	2.90	0.013
2Sb/900 °C						
15 min	1.3	2.58	0.008	2.00	2.88	0.014
1 h	1.7	2.57	0.011	1.7	2.88	0.014
4 h	1.3	2.58	0.006	2.0	2.87	0.012
5Sb/900 °C						
15 min	1.4	2.60	0.010	1.9	2.89	0.014
4 h	1.7	2.59	0.006	1.5	2.88	0.012
1000 °C						
30 s	1.6	2.56	0.006	1.6	2.86	0.012
10 min	2.0	2.57	0.008	0.9	2.88	0.014

C. EXAFS

The EXAFS experiments[6] have been carried out at the wiggler station 9.3 of the Daresbury synchrotron (U.K.). Near grazing incidence geometry fluorescence EXAFS have been performed at the Sb K edge (30 491 eV). The incident angle was approximately twice the Si critical angle (70 mdeg at this energy). Hence, the x-ray penetration depth is approximately 500 nm, which is larger than the thickness of the Sb and B layers. Therefore, the whole implanted layer is probed during these EXAFS experiments. The high x-ray energy used explains that very few similar experiments have been carried out. To our knowledge, only Van Netten, Stapel, and Niesen[7] have performed similar EXAFS experiments on a 70 ppm Sb-implanted silicon crystal. The harmonic rejection rate was approximately 50%. The fluorescence detector used is a Canberra 13 Ge diode detector with an excellent signal-to-noise ratio due to its energy discrimination (the energy resolution is about 100 eV at 10 keV). As the samples are monocrystalline, this device is also useful to eliminate Bragg peaks present in the EXAFS spectra. The signals from the different detectors are summed all together after removal of the spectra with Bragg peaks. Several scans have been performed for each sample in order to improve the statistics.

For the analysis, the first reference sample used is a metallic Sb foil for the Sb–Sb backscattering amplitude and phase data. This reference is appropriate because at high annealing temperature, many Sb-implanted atoms are present in precipitates having the metallic Sb rhombohedric structure. In this structure, each Sb atom has three first nearest neighbors (NNs) at 2.90 Å and three second NNs at 3.36 Å.[8] The second reference used is a 2×10^{16} Sb^+ and B^+/cm^2 laser annealed sample, for which it is assumed that each Sb atom is surrounded by four Si neighbors. Indeed, after laser annealing the Sb atoms are in substitutional sites up to a concentration of approximately 2×10^{21} atoms/cm^3.[9] After thermal annealing, the concentration of free carriers decreases, and the impurity evolves into a more stable state leading to the formation of precipitates or complexes.[3,5,10] Bechstedt and Harrison[11] have estimated theoretically that the Sb–Si distance in the substitutional approximation is 2.52 Å.

The EXAFS spectra have been analyzed using the spherical wave program EXCURV92.[12] Actually, the B atom looks like a vacancy regarding the EXAFS analysis. This has been confirmed by comparing the simulated EXAFS spectra using the EXCURV theoretical backscattering amplitudes and phases of an Sb atom surrounded by either three Si atoms and one B atom or three Si atoms and one vacancy. No difference has been found between the two situations. Therefore, no direct information is obtained for the Sb—B bond. Anyhow, it is shown that the influence of B can be seen through the number of Sb atoms in precipitates.

The absorption spectra have been analyzed as follows: The spectrum background has been removed by extrapolating the pre-edge region by a first-order polynomial. The wave-vector origin is taken at the inflexion point of the spectrum. The Fourier transforms (FTs) have been performed in the 2.5–10.5 Å^{-1} K range. Theoretical potentials in the X_α model have been used. The total number of independent parameters from the Nyquist theorem is 9. Hence, both contributions Sb–Si and Sb–Sb for the NN can be determined.

III. RESULTS

A. EXAFS results

The number and coordination distances of the Si and Sb first neighbors are reported in Table I, together with the corresponding Debye–Waller (DB) factors.

For the 2Sb samples, Sb atoms are surrounded by approximately three Sb atoms at 2.90 Å, whatever the annealing period. This first NN number and distance are in good agreement with the Sb–Sb distance in the metallic rhombohedral Sb structure. From the corresponding FTs [see Fig.

Downloaded 15 Nov 2012 to 155.69.4.4. Redistribution subject to AIP license or copyright; see http://jap.aip.org/about/rights_and_permissions

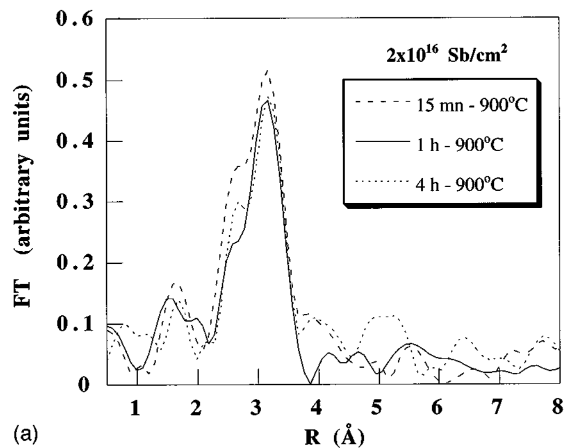

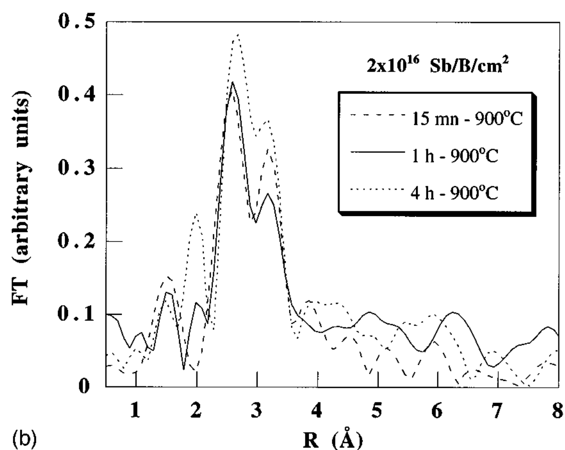

FIG. 1. FT of the (a) 2Sb and (b) 2SbB samples annealed at 900 °C.

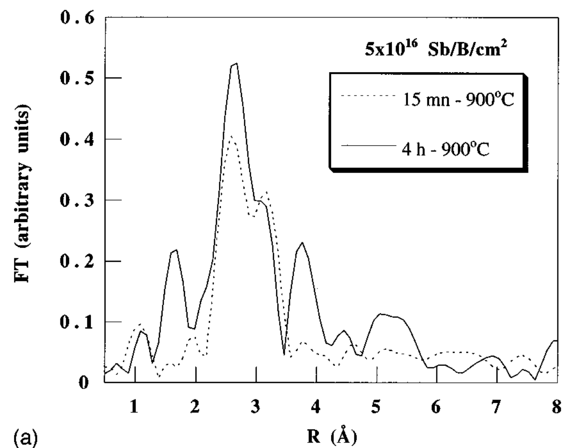

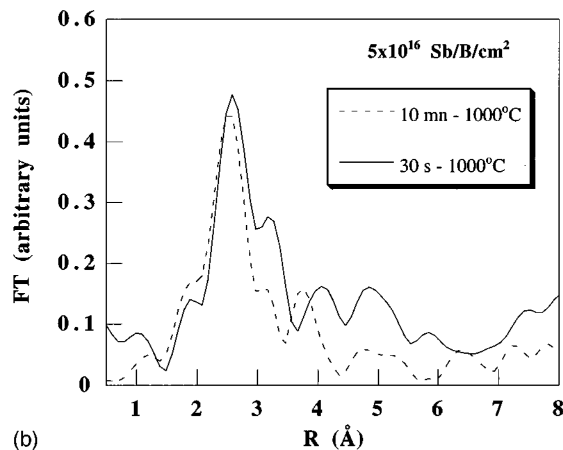

FIG. 2. FT of the 5SbB samples annealed at (a) 900 °C and (b) 1000 °C.

1(a)], one can remark that there is no pronounced long-distance order except for the longest (4 h) annealing time. The DW factor for these specimens is found to be equal or slightly larger than the value of metallic Sb given to be 0.012 $Å^2$. The DW values seem to indicate that the NN shell is better ordered for a short annealing time (15 min). For the 2SbB samples [FT in Fig. 1(b)], Sb atoms are surrounded by both Si and Sb atoms at approximately 2.58 and 2.88 Å, respectively. The experimental Sb–Si distance obtained in the studied samples lies in between the 2.53 Å value found by Van Netten and co-workers[7] in a 70 ppm Sb-doped Si sample and the Sb–Si distance in an amorphous sample (2.60 Å).[4] This may be explained by an incomplete crystal regrowth. The Sb–Si DW factor for these specimens is found to be slightly smaller than the bulk Si one which is 0.01 $Å^2$. One can realize that an Sb atom in a Si matrix can not move a lot because of its large volume and weight: It acts as a defect for phonon propagation and can be a knot for this wave. The DW factors suggest that the NN shell is more ordered for the long annealing time (4 h). This phenomenon is in opposition with the one obtained for the 2Sb samples. Moreover, the poor order at longer distance remains globally the same as the annealing time increases.

Moreover, let us point out a peculiar phenomenon: For Sb implanted in Si, the dopant has three Si neighbors at 2.60 Å in the amorphized layer after implantation and four Si neighbors at 2.54 Å in substitutional position. On the contrary, for As, the NN distance has been observed smaller for the amorphous case (2.38 Å) than for the substitutional one (2.41 Å).[13] Indeed, it has been found that the As and Sb substitutional donors occupy nearly the same volume of the Si atom in the lattice.[14] Hence, the Sb–Si substitutional distance is proportionally smaller than the As one.

For the 5SbB samples annealed at 900 °C [FT in Fig. 2(a)], Sb atoms are surrounded by Si and Sb atoms at approximately 2.60 and 2.88 Å, respectively. The first NN number varies, with the annealing period, between 1.4 and 1.7 for Si neighbors and between 1.9 and 1.5 for Sb neighbors. From the DW factors, one can see that the first NN shell is better ordered for the long annealing time (4 h). As time increases, the short-range order improves.

For the 5SbB samples annealed at 1000 °C, Sb atoms are surrounded by Si and Sb atoms at approximately 2.56 and 2.87 Å, respectively. From the DW factors, the NN shell is better ordered for a short annealing period. From the corresponding FTs [see Fig. 2(b)], one can see that the long-distance order is better for the 10 min annealing period than for a shorter one (30 s).

B. Absorption edge jump at the Sb *K* edge

The absorption edge jump is proportional to the number of probed atoms. For a given annealing temperature the edge

Downloaded 15 Nov 2012 to 155.69.4.4. Redistribution subject to AIP license or copyright; see http://jap.aip.org/about/rights_and_permissions

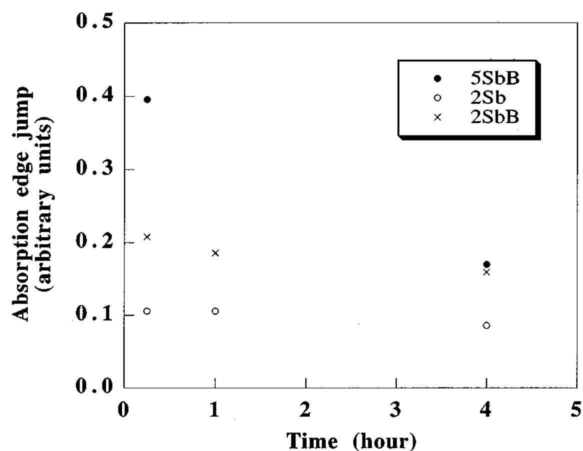

FIG. 3. Evolution of the absorption edge jump obtained from x-ray absorption spectra vs annealing time at 900 °C (10% uncertainty).

jump varies with the implantation types (Sb or Sb and B) and with the annealing time. A reduction in the jump ratio is given by a phenomenon of antimony diffusion. The behavior of this parameter in the case of annealing at 900 °C is shown in Fig. 3. For the Sb only implanted samples, the absorption edge jump is the smallest one of the studied specimens and remains approximately constant when the annealing period increases. For the 2SbB samples, the absorption edge jump is twice larger than for the previous case. This is clearly due to the presence of B atoms, which prevents the Sb outdiffusion. Its value remains also approximately constant as the annealing period increases. For the 5SbB samples annealed at 900 °C, the absorption edge jump is twice larger than for the previous case (instead of 2.5 times larger according to the dose values) for a short annealing period (15 min). The absorption edge jump drops by a factor of 2.4 as the annealing time increases by a factor of 16 (from 15 min to 4 h). The corresponding amounts of outdiffused dopants are in agreement with the ones that can be deduced from the direct measurements of the Sb dose performed by RBS and reported in Table II, together with the corresponding values of the B dose deduced from NRA experiments. This table also shows that even a more dramatic outdiffusion occurs for the 5SbB samples, annealed at 1000 °C.

A previous study concerning the Sb diffusion in samples implanted with 2 and 5×10^{16} ions/cm^2 and annealed at a lower temperature (i.e., 600 °C) put also in evidence a high Sb outdiffusion.[5,15] This effect has been related to a high diffusivity close to the surface, due to lattice defects (e.g., twins, dislocations, rodlike defects) evidenced by transmission electron microscopy (TEM) observations.

TABLE II. B and Sb doses as determined from NRA and RBS, respectively. (Accuracy statistic 1% and systematic 6%.)

	B dose ($\times10^{16}$ cm^{-2})	Sb dose ($\times10^{16}$ cm^{-2})
2SbB as implanted	1.98	2.28
2SbB 900 °C, 15 min	1.62	2.24
2SbB 900 °C, 1 h	1.80	2.12
2SbB 900 °C, 4h	1.47	2.11
5SbB as implanted	4.80	5.66
5SbB 1000 °C, 30 s	5.04	2.28
5SbB 1000 °C, 10 min	5.15	1.41
5SbB 900 °C, 15 min	3.69	5.30
5SbB 900 °C, 4 h	4.67	1.98

TABLE III. Sb percentage in precipitates as determined by EXAFS with an uncertainty of 10%.

Samples	Sb precipitates (%)
2Sb/900 °C	
15 min	93
1 h	100
4 h	90
2SbB/900 °C	
15 min	67
1 h	57
4 h	67
5SbB/900 °C	
15 min	63
4 h	50
1000 °C	
30 s	53
10 min	30

C. Sb precipitation

The Sb atoms can be located in substitutional sites, complexes, and precipitates. The percentage of Sb atoms in precipitates can be easily deduced from $N_{\mathrm{Sb-Sb}}$ as each Sb atom in a precipitate has three Sb neighbors. The precipitate percentages are summarized in Table III.

For the 2Sb samples, nearly all Sb atoms are in precipitates, even after a short annealing treatment (15 min at 900 °C). This is in good agreement with a previous work,[16] where RBS measurements suggested a significant Sb precipitation for 1×10^{16} Sb/cm^2 samples annealed at 850–1000 °C (a substitutional fraction was found to be less than 10%).

For the 2SbB samples, approximately two-thirds of the Sb atoms are in precipitates; hence, by comparison with the previous case, the presence of B atoms slows down the Sb precipitation. This phenomenon occurs at the beginning of the annealing (before 15 min) and remains quite stable over a long annealing period (at least up to 4 h).

For the 5SbB samples annealed at 900 °C, the percentage of Sb precipitates is similar to the previous case (lower dose) for a short annealing period.

IV. DOPANT PROFILE SIMULATION

The EXAFS results on the Sb precipitation have been compared with the ones deduced from a numerical simulation. This program describes the evolution of the dopant profiles during annealing, taking into account the precipitation of both Sb and B, as well as the Sb–B pairing, therefore, it enables one to obtain the fraction of Sb atoms in substitutional sites, complexes, and precipitates. Its ability to model the donor and acceptor codiffusion has been checked in previous articles.[5,17]

Downloaded 15 Nov 2012 to 155.69.4.4. Redistribution subject to AIP license or copyright; see http://jap.aip.org/about/rights_and_permissions

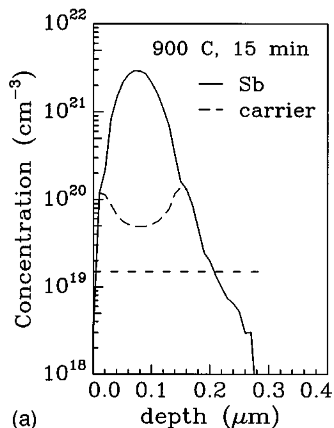

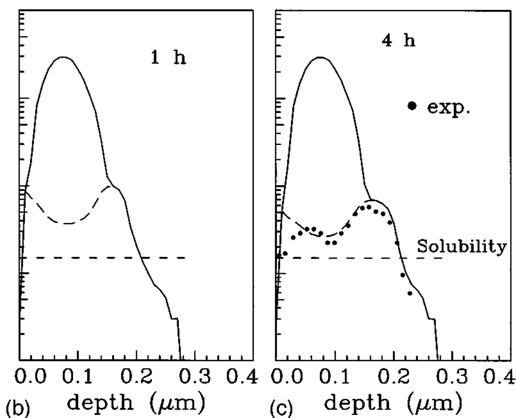

FIG. 4. Simulation of the Sb and carrier concentration profiles of the 2Sb samples annealed at 900 °C for (a) 15 min, (b) 1 h, and (c) 4 h. In the case of 4 h, the corresponding experimental carrier profile is also reported. The solubility value is also shown for comparison (Ref. 1).

For Sb only implanted samples, we have used the model described in Refs. 18 and 19, which solves the diffusion equations, taking into account the Sb precipitation for concentrations exceeding the solubility value, according to the theory of homogeneous nucleation and of the diffusion-limited growth of the particles. In this way, both the total and the precipitate Sb profiles are obtained, wherefrom the electrically active substitutional dopant profile can be computed. The results of the simulation of the 2Sb samples, annealed at 900 °C for the different times, are shown in Figs. 4(a)–4(c). At this temperature the solubility of Sb in Si is 1.5×10^{19} cm^{-3}.[1] Due to the strong supersaturation, a fraction of the dopant already precipitates during the fast epitaxial regrowth of the amorphous implanted layer. During this process, the Sb atoms occupy substitutional sites up to a concentration of about 3.5×10^{20} cm^{-3},[18] then the precipitation continues with the annealing time, 95% of Sb atoms being already precipitated after 15 min at 900 °C, 96% after 1 h and 97% after 4 h. Due to the low Sb diffusivity, the equilibrium is not even reached after 4 h, as can be deduced from the comparison between the carrier profile and the solubility value in Fig. 4(c). The quality of the simulation is demonstrated by the good agreement between the carrier profile and the experimental data, previously obtained in a similar sample[20] and reported in the same figure. The above-reported fractions of precipitates are in good agreement with the corresponding ones obtained by the EXAFS measurements (Table III).

For the 2SbB samples the simulations are performed according to the model which takes into account the pairing between donors and acceptors.[5,17] The chemical reaction

$$Sb^{+}+B^{-}\Leftrightarrow SbB \qquad (1)$$

which leads to the formation of neutral pairs from isolated ions is considered.

The reaction is governed by the mass action law

$$\Omega C_{B}C_{Sb}=C_{pair}, \qquad (2)$$

where C_B and C_{Sb} are the concentration of B and Sb in the silicon lattice, thus available for the reaction, C_{pair} the pair concentration, and Ω the equilibrium constant of the reac-

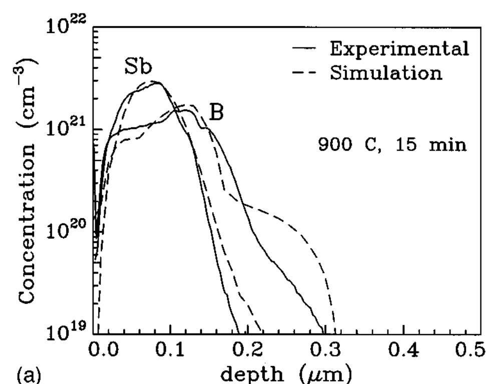

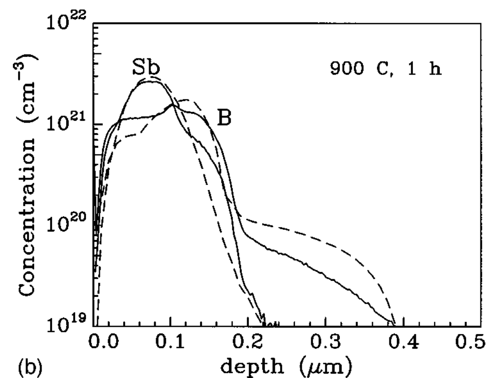

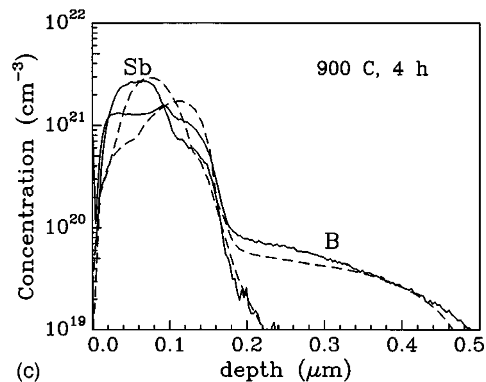

FIG. 5. Comparison between SIMS and simulated Sb and B concentration profiles of the 2SbB samples annealed at 900 °C for (a) 15 min, (b) 1 h, and (c) 4 h.

Downloaded 15 Nov 2012 to 155.69.4.4. Redistribution subject to AIP license or copyright; see http://jap.aip.org/about/rights_and_permissions

tion. Three coupled diffusion equations are used to describe the behavior of Sb, B, and pairs.[5,17] The precipitation of both Sb and B is also considered.

The simulation results of the samples 2SbB annealed at 900 °C for the same times are shown in Figs. 5(a)–5(c), where for comparison the corresponding SIMS profiles are also reported. The agreement between experimental and simulated profiles is quite satisfactory, if one takes into account the very high dopant concentration and the number of competing phenomena, which operate at the same time (phase transformations, pairing reaction, electrical compensation). For instance, the simulated B profiles show the typical shoulder which is present in the experimental ones, as due to the presence of immobile precipitated dopant. For the longest annealing treatment, this shoulder occurs at a concentration which corresponds to the equilibrium value [6.7×10^{19} cm^{-3} at 900 °C (Ref. 21)]. The fraction of Sb precipitates is about 60% and keeps constant by increasing the annealing time, in agreement with the results obtained by EXAFS (Table III).

V. CONCLUSIONS

The local atomic environment of Sb in 2 and 5×10^{16} ions/cm^2 implanted Si samples has been studied by near grazing incidence fluorescence EXAFS. The most striking result is the strong Sb out-diffusion in the Sb only implanted samples and annealed at high temperature (900 °C) even for a small time (15 min). At this stage, nearly all the Sb atoms are in precipitates. In the Sb–B coimplanted samples, the Sb out-diffusion decreases by a factor of 2 and the Sb percentage in precipitates is reduced by approximately one-third. Also, as the thermal annealing is more complete, the Sb percentage in precipitates is smaller. Moreover, the Sb and B profiles in the Si matrix have been simulated and excellent agreement is found between the theoretical percentage of Sb precipitates and the experimental data.

ACKNOWLEDGMENTS

The authors wish to thank A. Vandrot for the Sb and B implantation, P. Negrini for the annealing treatments, A. Dent for his efficient assistance at the station 9.3 at Daresbury, and A. Demourgues for his great help.

[1] D. Nobili, R. Angelucci, A. Armigliato, E. Landi, and S. Solmi, J. Electrochem. Soc. **136**, 1142 (1989).
[2] D. Nobili, in *Semiconductor Silicon 1990*, edited by H. Huff, Barraclough, and Onikawa (The Electrochemical Society, Princeton, NJ, 1990), Vol. 90-7.
[3] A. N. Larsen, F. T. Pedersen, G. Weyer, R. Galloni, R. Rizzoli, and A. Armigliato, J. Appl. Phys. **59**, 1908 (1986).
[4] J. L. Allain, A. Bourret, J. R. Regnard, and A. Armigliato, Appl. Phys. Lett. **61**, 264 (1992).
[5] B. Margesin, R. Canteri, S. Solmi, A. Armigliato, and F. Baruffaldi, J. Mater. Res. **6**, 2353 (1991).
[6] C. Brizard, J. R. Regnard, and A. Demourgues, Physica B **208&209**, 474 (1995).
[7] T. J. Van Netten, K. Stapel, and L. Niesen, J. Phys. (Paris) C **8**, 1049 (1986).
[8] R. W. G. Wyckoff, *Crystal Structures* (R. E. Krieger, Huntington, NY, 1982).
[9] R. Stuck, E. Fogarassy, J. Grob, and P. Siffert, Appl. Phys. **23**, 15 (1980).
[10] E. Antoncik, Nucl. Instrum. Methods B **12**, 219 (1985).
[11] F. Bechstedt and W. A. Harrison, Phys. Rev. B **39**, 5041 (1989).
[12] S. J. Gurman, N. Binsted, and I. Ross, J. Phys. C **17**, 143 (1984).
[13] J. L. Allain, J. R. Regnard, A. Bourret, A. Parisini, A. Armigliato, G. Tourillon, and S. Pizzini, Phys. Rev. B **46**, 9434 (1992).
[14] D. Sasireka and E. Palaniyandi, Phys. Rev. B **46**, 2047 (1992).
[15] A. Armigliato, F. Romanato, A. Drigo, A. Carnera, C. Brizard, J. R. Regnard, and J. L. Allain, Phys. Rev. B **52**, 1859 (1995).
[16] J. S. Williams and K. T. Short, J. Appl. Phys. **53**, 8663 (1982).
[17] S. Solmi, S. Valmorri, and R. Canteri, J. Appl. Phys. **77**, 2400 (1992).
[18] S. Solmi, F. Baruffaldi, and M. Derdour, J. Appl. Phys. **71**, 696 (1992).
[19] S. Solmi, E. Landi, and F. Baruffaldi, J. Appl. Phys. **68**, 3250 (1990).
[20] S. Solmi (unpublished).
[21] A. Armigliato, D. Nobili, P. Ostoja, M. Servidori, and S. Solmi, in *Semiconductor Silicon 1977*, edited by H. Huff and E. Sirtl (The Electrochemical Society, Princeton, NJ, 1977), Vol. 77-2, p. 88.

Downloaded 15 Nov 2012 to 155.69.4.4. Redistribution subject to AIP license or copyright; see http://jap.aip.org/about/rights_and_permissions